Microfluidics-Integrated Microwave Sensors for Single Cells Size Discrimination

Arda Secme[1]
[1]*Department of Mechanical Engineering,* Bilkent University, Ankara, Turkey
arda.secme@bilkent.edu.tr

Hadi Sedaghat Pisheh[1]
[1]*Department of Mechanical Engineering,* Bilkent University, Ankara, Turkey
hadi.sedaghat@bilkent.edu.tr

H. Dilara Uslu[1]
[1]*Department of Mechanical Engineering,* Bilkent University, Ankara, Turkey
dilara.uslu@bilkent.edu.tr

Ozge Akbulut[2]
[2]*Department of Molecular Biology and Genetics,* Bilkent University, Ankara, Turkey
o.akbulut@bilkent.edu.tr

R. Tufan Erdogan[1]
[1]*Department of Mechanical Engineering,* Bilkent University, Ankara, Turkey
tufan.erdogan@bilkent.edu.tr line

M. Selim Hanay[1,3*]
[1]*Department of Mechanical Engineering,*[3]*National Nanotechnology Research Center (UNAM)* Bilkent University, Ankara, Turkey
selimhanay@bilkent.edu.tr

2020 IEEE MTT-S International Microwave Biomedical Conference (IMBioC) | 978-1-7281-5866-2/20/$31.00 ©2020 IEEE | DOI: 10.1109/IMBIOC47321.2020.9385048

***Abstract*— The size of a cell is one of the most fundamental biophysical parameters it possesses. Traditionally size measurements are done by using optical microscopy and quantitative phase imaging. However, a sensor with higher resolution, high throughput and lower cost is still needed. Here, a novel microfluidics-integrated microwave sensor is demonstrated to characterize single cells in real-time without labelling. Coplanar waveguide resonator is designed with a bowtie-shaped sensing electrodes separated by 50 µm. Cells are transported to sensing region by microfluidic channels and their sizes are measured simultaneously by the microwave sensors and optical microscopy. To enhance the microwave resolution, the microwave resonator is equipped with external heterodyne measurement circuitry detecting each and every cell passing through the sensing region. By comparing quantitative microscopic image analysis with frequency shifts, we show that microwave sensors can effectively measure cellular size. Our results indicate that microfluidics-integrated microwave sensors (MIMS) can be used for detecting.**

Keywords— cell size, microwave resonators, MIMS

I. INTRODUCTION (*HEADING 1*)

Precise measurements of cellular size at high speed have opened up avenues for personalized medicine and early diagnosis of diseases [1,2]. To measure cellular size, quantitative phase microscopy [1,3,4] can be used to trap a cell and continuously observe its dynamics. However, for point-of-care applications, a system with a smaller form factor, cost and ease of use is needed. Among the advances with microscale sensors include the observation of fast mass fluctuations at the single cell scale [5] and measurement of differential drug response of cancer cells derived from different patients [6]. Remarkably, mass is not the only parameter suitable for determining the total material content inside a cell. As cells synthesize more biochemical components, such as cytoskeletal proteins and phospholipids, and maintain an imbalance of different electrolytes in their cytosols with respect to the external medium, their total electrical polarizability are expected to become markedly different than the polarizability of its external environment. Therefore, an electrical sensor capable of resolving minutiae capacitance changes induced by a single cell can be used for sizing single cells, in principle. However, at low electrical frequencies (smaller than ~1 GHz), extraneous effects such as Debye screening and cell membrane polarization dominates the response. Therefore, techniques working in this range, such as conventional impedance spectroscopy, do not directly yield cellular size. On the other hand, above ~ 1 GHz, electrolyte ions cannot follow the electromagnetic field and gets shorted out; however, hydrogen bonds in the water can still follow the polarization up to about 20 GHz [7]. As a result, a large contrast difference emerges between extracellular medium (mainly composed of water) and intracellular biopolymers (such as cytoskeleton and organelles) at the lower end of the microwave frequencies. This contrast difference enables microwave sensors with much larger dimensions to be used to measure cells compared to mechanical sensors [8-13]. In contrast to other MW resonators reported in the literature, the presented sensor benefits from real time frequency modulations continuously tracked with an custom built closed loop circuitry (PLL). Our phase sensitive detection system has much higher sensitivity (typically 1 part in 10^8) compared to the rest of microwave resonators that are directly measured by considering signal amplitude changes on a Vector Network Analyzer (VNA). "Fig. 1" shows the coplanar waveguide narrows down to 50 µm at the sensing region to obtain intense electric field to increase sensitivity of the detection ("Fig. 1-*a*"). As cells pass through the sensing region one by one, they induce distinct frequency shifts in the microwave sensor while at the same time imaged using optical microscopy ("Fig. 1-*b*").

978-1-7281-5866-2/20/$31.00 ©2020 IEEE

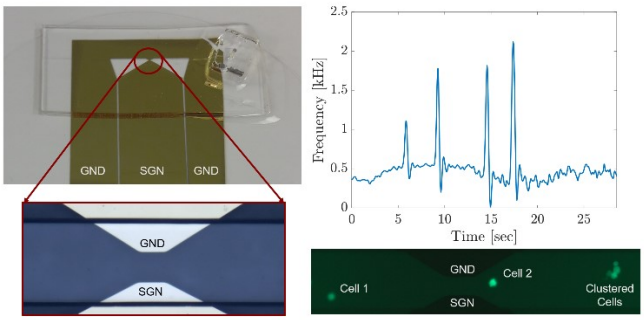

Fig. 1. (*a*) While electronic data is recorded, sensing electrodes, separated by 50 μm, is monitored under an optical microscope. (*b*) An example of frequency response of the resonator. Cells induce precipitous shift in the resonance that is proportional to the size of the cell.

II. Method

There are three main subsystems in the experimental: microwave measurement, optical microscope, and microfluidic controller. A custom made Phased Locked Loop (PLL) algorithm in LabVIEW is employed to lock the phase of the resonator to 0 degrees [14]. Initial characterization of our devices is done by Network Analyzer and since our device has a single SMA port, we used a circulator to find the resonance frequency via S21 (~ 2.5 GHz). A narrow-band detection scheme which is centered around the first resonance frequency of the CPW structure is employed to enhance the sensitivity of the measurement. Phase-sensitive detection is performed with a lock-in amplifier. Deviations from zero degrees outputs error and updates the drive frequency on the signal generator. With that, the resonator is constantly kept at its resonance frequency. As monolayer cells are easy to culture, we have incubated MDA-MB-231 LUC2 GFP cells. For experiments, the cells are trypsinized and detached from the culture plate. Suspended cells are kept in a reservoir and their medium is also added. While the sensing region is observed by the optical microscope (Zeiss, Axio Imager 2) cells are transported to the sensing region with a pressure controller (Fluigent).

The fabrication of the sensor chip involves two main steps: deposition of gold electrodes and microfluidic channel bonding. Gold electrode fabrication starts with exposing photoresist, coated on fused silica wafer, to UV light. After the desired pattern is developed, chips are coated with 120 nm gold by the thermal evaporation process. Two PDMS microchannel with dimensions, of 100 μm in width and 110 and 55 μm in depth, are plasma bonded on chip with the gold electrodes. Sensitive region of gold electrodes are aligned with microfluidic channel.

III. Results

Images obtained from the optical microscope are processed and area is measured by encapsulating the pixels forming the cell shape. The size of a single pixel is calculated by calibrating number of pixels with device dimensions and repetitive measurements give deviation in the cell size. The pixelated area is then converted first into actual area, and then assuming a spherical shape, into volume. By comparing the geometric volume obtained from the optical microscope and electrical volume of the cell which is measured by microwave signals and includes both geometric volume and unknown relative permittivity of the cell. We have seen a linear relationship between geometric and electric volume of a cell ("Fig. 2"). Bandwidth of the measurement is 2 Hz and some cells that passed much more rapidly than the bandwidth of the measurement were excluded from the data analysis.

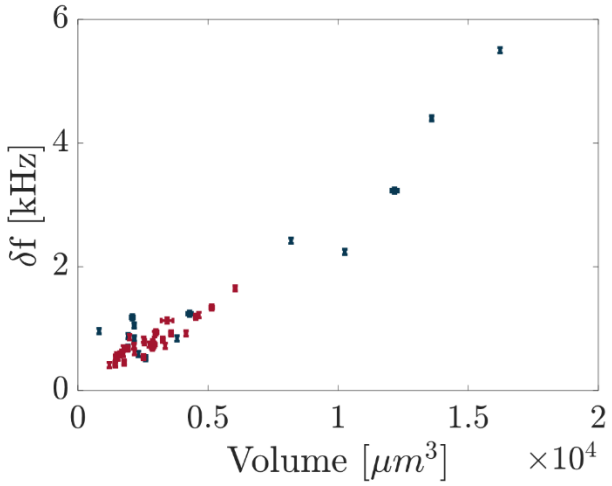

Fig. 2. Comparison of the optical volume of the cell and induced frequency shift. Red data points: cells passing through the middle of the channel without overlapping the electrodes. Blue data points: cell trajectory overlaps one of the electrodes. Here channel height is 110 μm.

For the cells that pass through the middle of the channel and hence do not overlap with the sensing electrodes (red data points in "Fig. 2"), the fitting to the linear trend is much stronger compared to the trend seen in cells whose trajectory overlaps the sensing electrodes (blue data points in "Fig. 2"). The sensitivity of the first sensor in "Fig. 2" is $3.3 \times 10^{-4}\ kHz/\mu m^3$ and noise floor is around 40Hz. The dispersion values for linear fit are: 0.11 and 0.46 for non-overlapping and overlapping cells, respectively and overall dispersion value is 0.27. The sensitivity of the second sensor, having channel height of 55 μm (not illustrated), is $1.2 \times 10^{-3}\ kHz/\mu m^3$ and noise floor is around 100 Hz. The dispersion values for linear fit are: 0.43 and 1.23 for non-overlapping and overlapping cells, respectively and overall dispersion value is 0.92. By reducing the channel height from 110 μm to 55 μm, we observed higher frequency shifts as cells pass closer to the sensing electrodes. To understand which electrode is more sensitive, we used the Sigma-Aldrich 20 μm polystyrene beads (Supelco - 74491) which are typically used as size standards. With second device having resonance frequency of 2.52 GHz, the same experimental procedure is repeated as with the cells and we spanned the locations along the width of the channel. Each particle is trapped near the sensing region and repeatedly moved it back and forth many times. To elucidate the trend, we obtained the statistics of eleven different particles, each of which transits the sensing region at a different position. "Fig. 3" shows the positional sensitivity of the sensor by partitioning its sensing region into eleven different locations. Shift in the resonance frequency turns out to be larger near the edge of ground electrode. The frequency responsivity reduces by more than half towards the

signal electrode. However, in between two electrodes, the frequency shifts are almost constant within the noise level ("Fig. 3"). This indicates that microwave measurements can be used for size measurements, without the need of additional microscope for position determination, as long as particle flow is confined within the central region which can be done through hydrodynamic focusing or modifying the device design.

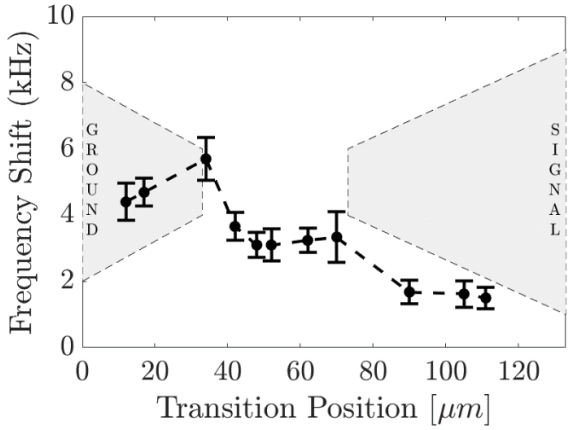

Fig. 3. Each data corresponds to the center of the 20 μm particle passing along. In between the sensing electrodes, amount of frequency shift remains on par with the noise level.

Once the single micro-particle experiments were done, we turned our attention to conducting single-cell trapping experiments. By fine-tuning the applied pressure dynamically, two different single cells is trapped and moved along the sensing electrodes.

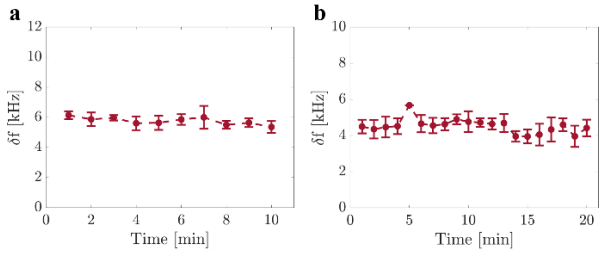

Fig. 4. Forward-Backward experiments with 2 different sized cells. Trend is investigated for each minute. For short period of time, frequency shifts remain stable.

The first cell, having mean area of 774 $\mu m^2 \pm 6.6\,\mu m^2$, is trapped for 10 minutes and trend in each minute is plotted ("Fig. 4-a"). The average frequency shift turns out to be 5.7 kHz with standard deviation of 0.5 kHz. For the second cell, which is smaller compared to first one and having area of 688 $\mu m^2 \pm 13.3\,\mu m^2$, forward backward motion is done for 20 minutes and average frequency shift turns around 4.5 kHz with standard deviation of 0.5 kHz ("Fig. 4-b"). With the proposed sensor technology, size of the same cell can be measured repeatedly and compared to frequency shift statistics.

IV. Conclusion

In this work, we have demonstrated how the frequency shift signal of microfluidics-integrated microwave sensors (MIMS) can be correlated to geometrical size of the single cells by correlating the microwave signal with optical microscopy measurements. As the correlation line has a non-negligible dispersion to understand the origin of it, we repeatedly measure the same particle or cell through the active sensing region. The result indicates that while the response is almost constant at the center of the channel, it starts to get skewed when the trajectory of the cell passes over the electrodes. The elimination of positional dependency, by designing sensing regions with more homogeneous electric fields, is one of the first priorities in MIMS technology. The sensor resolution is still at least an order of magnitude smaller than the similar techniques, however, considering their large sizes and recent introduction, a quick progress for reducing the sensor volume and eliminating noise processes is expected.

Acknowledgment

This work was supported by ERC Starting Grant *REM,* no: 758769.

References

[1] Mir, M. et al. "Optical measurement of cycle-dependent cell growth," Proceedings of the National Academy of Sciences 108, 13124-13129 (2011).

[2] Rosendahl, P. et al. "Real-time fluorescence and deformability cytometry," Nature methods 15, 355 (2018).

[3] Popescu, G. et al. "Optical imaging of cell mass and growth dynamics," American Journal of Physiology-Cell Physiology 295, C538-C544 (2008).

[4] Park, Y., Depeursinge, C. & Popescu, G. "Quantitative phase imaging in biomedicine," Nature Photonics 12, 578 (2018).

[5] Martínez-Martín, D. et al. "Inertial picobalance reveals fast mass fluctuations in mammalian cells," Nature 550, 500 (2017).

[6] Cetin, A. E. et al. "Determining therapeutic susceptibility in multiple myeloma by single-cell mass accumulation," Nat. Commun. 8, 1613 (2017).

[7] Chen, T. et al. in 2013 IEEE MTT-S International Microwave Symposium Digest (MTT). 1-4 (IEEE).

[8] Ferrier, G. A., Romanuik, S. F., Thomson, D. J., Bridges, G. E. & Freeman, M. R. "A microwave interferometric system for simultaneous actuation and detection of single biological cells," Lab on a Chip 9, 3406-3412 (2009).

[9] Nikolic-Jaric, M. et al. "Microwave frequency sensor for detection of biological cells in microfluidic channels," Biomicrofluidics 3, 034103 (2009).

[10] Yang, Y. et al."Distinguishing the viability of a single yeast cell with an ultra-sensitive radio frequency sensor," Lab on a Chip 10, 553-555 (2010).

[11] Dalmay, C. et al. "Ultra sensitive biosensor based on impedance spectroscopy at microwave frequencies for cell scale analysis," Sensors and Actuators A: Physical 162, 189-197 (2010).

[12] Chien, J.-C. et al. "A high-throughput flow cytometry-on-a-CMOS platform for single-cell dielectric spectroscopy at microwave frequencies," Lab on a Chip 18, 2065-2076 (2018).

[13] Watts, C. et al. "Microwave Dielectric Sensing of Free-Flowing, Single, Living Cells in Aqueous Suspension," IEEE Journal of Electromagnetics, RF and Microwaves in Medicine and Biology (2019).

[14] Kelleci, M., Aydogmus, H., Aslanbas, L., Erbil, S. O. & Hanay, M. S. "Towards microwave imaging of cells," Lab on a Chip 18, 463-472 (2018).